

A low-noise, high-SNR balanced homodyne detector for the bright squeezed state measurement in 1-100 kHz range

Jin-Rong Wang(王锦荣), Qing-Wei Wang(王庆伟), Long Tian(田龙), Jing Su(苏静), Yao-Hui Zheng(郑耀辉)

Citation: Chin. Phys. B . 2020, 29(3): 034205 . **doi:** 10.1088/1674-1056/ab683b
Journal homepage: http://cpb.iphy.ac.cn; http://iopscience.iop.org/cpb

What follows is a list of articles you may be interested in

Optical enhanced interferometry with two-mode squeezed twin-Fock states and parity detection

Li-Li Hou(侯丽丽), Shuai Wang(王帅), Xue-Fen Xu(许雪芬)

Chin. Phys. B . 2020, 29(3): 034203 . **doi:** 10.1088/1674-1056/ab6837

Double-passage mechanical cooling in a coupled optomechanical system

Qing-Xia Mu(穆青霞), Chao Lang(郎潮), Wen-Zhao Zhang(张闻钊)

Chin. Phys. B . 2019, 28(11): 114206 . **doi:** 10.1088/1674-1056/ab48f1

Quantum optical interferometry via general photon-subtracted two-mode squeezed states

Li-Li Hou(侯丽丽), Jian-Zhong Xue(薛建忠), Yong-Xing Sui(眭永兴), Shuai Wang(王帅)

Chin. Phys. B . 2019, 28(9): 094217 . **doi:** 10.1088/1674-1056/ab38a9

Quantum interferometry via a coherent state mixed with a squeezed number state

Li-Li Hou(侯丽丽), Yong-Xing Sui(眭永兴), Shuai Wang(王帅), Xue-Fen Xu(许雪芬)

Chin. Phys. B . 2019, 28(4): 044203 . **doi:** 10.1088/1674-1056/28/4/044203

Effects of the Casimir force on the properties of a hybrid optomechanical system

Yi-Ping Wang(王一平), Zhu-Cheng Zhang(张筑城), Ya-Fei Yu(於亚飞), Zhi-Ming Zhang(张智明)

Chin. Phys. B . 2019, 28(1): 014202 . **doi:** 10.1088/1674-1056/28/1/014202

A low-noise, high-SNR balanced homodyne detector for the bright squeezed state measurement in 1–100 kHz range*

Jin-Rong Wang(王锦荣)[1], Qing-Wei Wang(王庆伟)[1], Long Tian(田龙)[1,2], Jing Su(苏静)[1,2], and Yao-Hui Zheng(郑耀辉)[1,2,†]

[1] *State Key Laboratory of Quantum Optics and Quantum Optics Devices, Institute of Opto-Electronics, Shanxi University, Taiyuan* 030006, *China*
[2] *Collaborative Innovation Center of Extreme Optics, Shanxi University, Taiyuan* 030006, *China*

(Received 4 October 2019; revised manuscript received 5 December 2019; accepted manuscript online 7 January 2020)

We report a low-noise, high-signal-to-noise-ratio (SNR) balanced homodyne detector based on the standard transimpedance amplifier circuit and the inductance and capacitance combination for the measurement of the bright squeezed state in the range from 1 kHz to 100 kHz. A capacitance is mounted at the input end of the AC branch to prevent the DC photocurrent from entering the AC branch and avoid AC branch saturation. By adding a switch at the DC branch, the DC branch can be flexibly turned on and off on different occasions. When the switch is on, the DC output provides a monitor signal for laser beam alignment. When the switch is off, the electronic noise of the AC branch is greatly reduced at audio-frequency band due to immunity to the impedance of the DC branch, hence the SNR of the AC branch is significantly improved. As a result, the electronic noise of the AC branch is close to −125 dBm, and the maximum SNR of the AC branch is 48 dB with the incident power of 8 mW in the range from 1 kHz to 100 kHz. The developed photodetector paves a path for measuring the bright squeezed state at audio-frequency band.

Keywords: quantum optics, photodetector, low-noise, audio band

PACS: 42.50.–p, 85.60.Gz **DOI:** 10.1088/1674-1056/ab683b

1. Introduction

Squeezed states are usually divided into two types: one is the bright squeezed state that has a coherent amplitude, and the other is the squeezed vacuum state that has no coherent amplitude.[1–5] Which type of squeezed light is desirable is dependent on the applications. In interferometer, the squeezed vacuum state is usually used to reduce the cross-interference influence due to no coherent amplitude.[6–10] While the bright squeezed state has a coherent amplitude, which can be used in spectroscopic measurement,[11,12] velocimetry,[13] LIDAR,[14] and quantum key distribution.[15,16]

The detection,[17,18] besides the generation[19–22] and propagation of squeezed states, is another key element for improving their application performances. Many dedicated researches have been carried out to explore a balanced homodyne detector (BHD) with low-noise, high-gain, and high common mode rejection ratio (CMRR).[23–30] Our group has designed a low-noise, high-gain photodetector based on the bootstrap structure with a clearance of 21 dB for 410 μW injected power.[25] Subsequently, by adopting a junction field-effect transistor (JFET) buffering input, we suppressed further the electronic noise of the photodetector, extended the dynamic range to 11.22 mW with a clearance of 36 dB.[29] Furthermore, by adding the differential fine turning circuit between two photodiodes (PDs), a maximum CMRR of 75.2 dB was obtained.[27] A common feature of these detectors described above is to employ a transimpedance amplifier (TIA), which is a natural choice for low-noise, shot-noise detection. In combination with the inductance and capacitance (*L*–*C*) circuit, the AC and DC signals are observed individually with different gains. The design, which is usually adopted to detect squeezed states at MHz regime, can not only prevent the DC signal from entering the AC branch that avoids AC branch saturation, but also provide a monitor signal for laser beam alignment. However, as the detection frequency decreases, the AC separation from the DC signal faces a challenge. In order to resolve the trouble, the DC coupled transimpedance detector is widely used to measure squeezed vacuum states at audio-frequency band. Vahlbruch *et al.* designed a DC coupled transimpedance detector, whose SNR is around 20 dB in the tens of Hertz to tens of thousands of Hertz frequency band for optical power of around 1 mW.[31] Compared with the squeezed vacuum state, the bright squeezed state with coherent amplitude can not be accurately detected by the DC coupled transimpedance detector due to the saturation effect. Therefore, one challenge, that is the particular focus of this paper, is the construction of a detection system for the bright squeezed state at audio-frequency band.

*Project supported by the National Natural Science Foundation of China (Grant Nos. 11654002, 61575114, 11874250, and 11804207), the National Key Research and Development Program of China (Grant No. 2016YFA0301401), the Program for Sanjin Scholar of Shanxi Province, China, the Program for Outstanding Innovative Teams of Higher Learning Institutions of Shanxi, China, the Fund for Shanxi "1331 Project" Key Subjects Construction, China, and Key Research and Development Projects of Shanxi Province, China (Grant No. 201903D111001).

†Corresponding author. E-mail: yhzheng@sxu.edu.cn

© 2020 Chinese Physical Society and IOP Publishing Ltd

In this paper, we design a low-noise, high-SNR BHD for the bright squeezed state measurement in the range from 1 kHz to 100 kHz. By using a capacitance to isolate the DC photocurrent from the AC amplification branch, the AC amplification branch of the photodetector is immune to saturation at audio-frequency band. By adopting a switch at the DC branch, the electronic noise of the AC branch is significantly reduced. At the same time, the intrinsic shunt of the DC branch at audio-frequency band is eliminated when the switch is off, hence the SNR of the AC branch is significantly increased. In addition, the DC branch does also provide a monitor signal for laser beam alignment when the switch is on. As a result, we obtain a high-performance BHD with the electronic noise of about −125 dBm, the maximum SNR of higher than 48 dB for 8 mW incident power, and the CMRR of higher than 59 dB in the range from 1 kHz to 100 kHz.

2. SNR analysis of the balanced homodyne detector

The main circuit diagram for the photodetector is shown in Fig. 1. Firstly, when the switch S is on, the DC photocurrent is enabled and amplified via an operational amplifier (Op-Amp, OP27) for laser beam alignment. When the switch S is off, only the AC photocurrent is amplified via TIA (ADA4817-1). Due to immunity to the impedance of the DC branch, the electronic noise of the AC branch is greatly reduced at audio-frequency band. A capacitance is mounted at the input end of the AC branch to prevent the DC photocurrent from entering the AC branch and avoid the AC branch saturation. The increase of the capacitance C_1 is benefit to obtaining lower cut-off frequency at the AC branch.[21] However, large capacitance C_1 can also introduce excess electronic noise. In this case, the capacitance C_1 of 47 μF is selected.

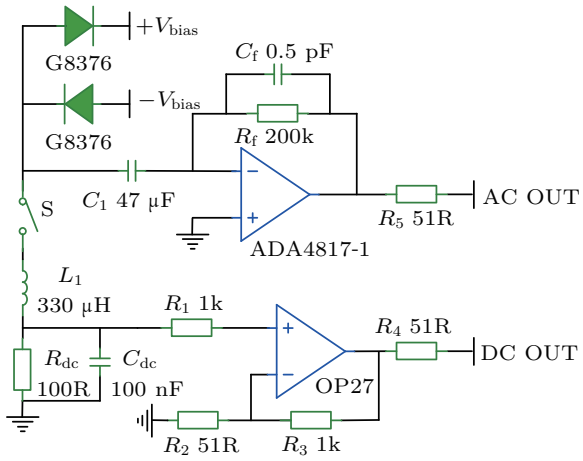


Fig. 1. The schematic of the BHD with *L*–*C* coupling and TIA circuit.

It is well-known that a large number of classical low-frequency noises[32] from the solid-state laser, external environment, and the BHD will inevitably be coupled into the detection system. Even though the balanced homodyne detection is an effective method to amplify the signal fluctuation and reduce the electronic noise, the electronic noise puts a stringent limit on the achievable SNR in the range from 1 kHz to 100 kHz. The model[27,28] for analyzing the AC output noise response of the BHD with TIA circuit is shown in Fig. 2. The dashed frames mark the impedance of the DC amplification branch and the equivalent circuits of the PDs, respectively.

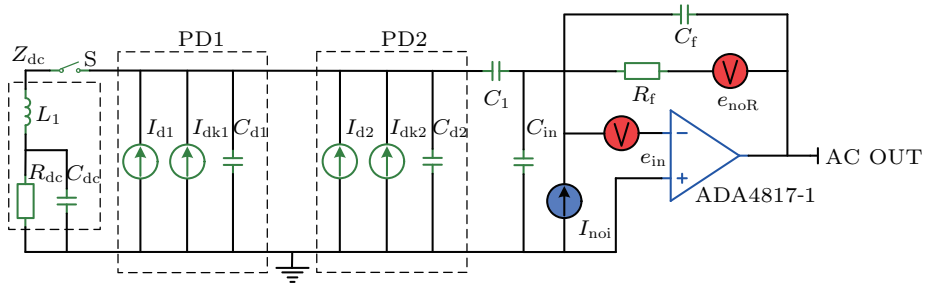


Fig. 2. The AC output noise response model of the photodetector. Some parameters are as follows: $I_{noi} = 2.5$ fA/$\sqrt{\text{Hz}}$, $I_{dk1} = I_{dk2} = 0.3$ nA, $C_{d1} = C_{d1} = 5$ pF, and $C_{in} = 1.4$ pF.

2.1. Electronic noise analysis

The electronic noise of the photodetector with *L*–*C* combination and TIA circuit can be classified into three parts:[33] one is from the feedback resistor, another is from the PD, and the third one is from Op-Amp.

The thermal noise caused by the feedback resistor R_f is given by

$$e_{R_f,\text{Thermal}} = \sqrt{4KT\Delta f/R_f} \cdot |Z_s|, \tag{1}$$

where K is the Boltzmann constant, T is the absolute temperature, and Δf is the unity measurement bandwidth. Z_s denotes the gain impedance of the TIA circuit, which is given by

$$Z_s = R_f \parallel (1/\text{j}2\pi f C_f), \tag{2}$$

where C_f is the feedback capacitance, f is the analysis frequency, and two parallel vertical bars $\parallel$ represent two components in parallel. In order to simplify these expressions in the following section, all of these components in parallel are represented by $\parallel$.

The electronic noise of the PD composes of the shot noise

caused by the dark current and the thermal noise generated by the shunt resistor. Given that the dark currents of the PD1 and PD2 are I_{dk1} and I_{dk2}, their induced shot noises $\Delta i_{PD1,Dark}$ and $\Delta i_{PD2,Dark}$ are written as

$$\Delta i_{PD1,Dark} = \sqrt{2qI_{dk1}\Delta f}, \tag{3}$$

$$\Delta i_{PD2,Dark} = \sqrt{2qI_{dk2}\Delta f}, \tag{4}$$

where q is the electronic charge. The shot noises induced by the dark currents of the PDs are too small to be taken into account compared to the thermal noise caused by the feedback resistor.

The thermal noises of the PD1 and PD2 can be expressed respectively in their current forms as follows:

$$\Delta i_{PD1,Thermal} = \sqrt{4KT\Delta f/R_{d1}}, \tag{5}$$

$$\Delta i_{PD2,Thermal} = \sqrt{4KT\Delta f/R_{d2}}, \tag{6}$$

where $R_{d1} = V_{bias}/I_{dk1}$ and $R_{d2} = V_{bias}/I_{dk2}$ are the shunt resistors of the PD1 and PD2, respectively. In the case of $V_{bias} = +5$ V, the thermal noise current is around 10 times lower than the shot noise of the dark current. Hence, the electronic noises of the PDs are not taken into account when calculating the electronic noise of the photodetector.

The electronic noise contribution from the Op-Amp includes two parts: the input current noise and the input voltage noise. If the input current noise of Op-Amp is I_{noi}, its equivalent contribution after the TIA is given by

$$e_{TIA,Current} = I_{noi} \cdot |Z_s| \cdot \sqrt{\Delta f}, \tag{7}$$

which can be neglected compared to the thermal noise caused by the feedback resistor in the range from 1 kHz to 100 kHz. Similarly, the electronic noise contribution from the input voltage noise of e_{in} is given by

$$e_{TIA,Voltage} = e_{in} \cdot |Z_n| \cdot \sqrt{\Delta f}, \tag{8}$$

where $|Z_n|$ represents the TIA voltage noise gain and is expressed as

$$Z_n = (Z_d + Z_s)/Z_d. \tag{9}$$

Here, Z_d includes two cases: $Z_{d,dc}$ and $Z_{d,no-dc}$, which respectively refer to the input impedances of the TIA circuit with and without the DC amplification branch and are expressed as

$$Z_{d,dc} = \frac{1}{j2\pi fC_{in}} \parallel \left(\frac{1}{j2\pi fC_1} + R_{d1} \parallel R_{d2} \parallel \frac{1}{j2\pi fC_{d1}} \parallel \frac{1}{j2\pi fC_{d2}} \parallel Z_{dc} \right), \tag{10}$$

$$Z_{d,no-dc} = \frac{1}{j2\pi fC_{in}} \parallel \left(\frac{1}{j2\pi fC_1} + R_{d1} \parallel R_{d2} \parallel \frac{1}{j2\pi fC_{d1}} \parallel \frac{1}{j2\pi fC_{d2}} \right), \tag{11}$$

where C_{d1}, C_{d2}, and C_{in} denote the junction capacitances of the PD1, PD2 and the input capacitance of the TIA circuit, respectively. Z_{dc} represents the equivalent impedance of the DC amplification branch and is given by

$$Z_{dc} = j2\pi fL_1 + (1/j2\pi fC_{dc}) \parallel R_{dc}. \tag{12}$$

Since all of the electronic noise terms (refer to Eqs. (1) and (8)) mentioned above are uncorrelated, the total electronic noise of the photodetector is given by

$$e_{EL,Noise} = \sqrt{e^2_{R_f,Thermal} + e^2_{TIA,Voltage}}. \tag{13}$$

By substituting Eqs. (1) and (8) into Eq. (13), the total electronic noise can be deduced as

$$e_{EL,Noise} = \sqrt{4KT/R_f \cdot |Z_s|^2 \cdot \Delta f + e^2_{in} \cdot |Z_n|^2 \cdot \Delta f}. \tag{14}$$

According to Eq. (14), the total electronic noises with and without the DC amplification branch can be calculated in the range from 1 kHz to 100 kHz in terms of the TIA parameters, which are shown in Fig. 3. It is worth noting that the inductance L and input voltage noise e_{in} differ in values for different frequencies in the range from 1 kHz to 100 kHz. The observed values in the frequencies of 1 kHz, 5 kHz, 20 kHz, 50 kHz, 70 kHz, 100 kHz are 32 mH, 3 mH, 500 μH, 348 μH, 344 μH, 342 μH and 12 nV/$\sqrt{\text{Hz}}$, 6 nV/$\sqrt{\text{Hz}}$, 5 nV/$\sqrt{\text{Hz}}$, 4.5 nV/$\sqrt{\text{Hz}}$, 4.3 nV/$\sqrt{\text{Hz}}$, 4 nV/$\sqrt{\text{Hz}}$, respectively. The results show that the electronic noise without DC amplification branch is far smaller than that with DC amplification branch. The reason is as follows: the thermal noise coming from the feedback resistor is a dominant source of the electronic noise without the DC amplification branch, the TIA voltage noise is dominant in the electronic noise with the DC amplification branch, and the thermal noise is far smaller than the TIA voltage noise. However, at MHz regime, the electronic noises with and without the DC amplification branch, which mainly come from the TIA voltage noise, are identical.

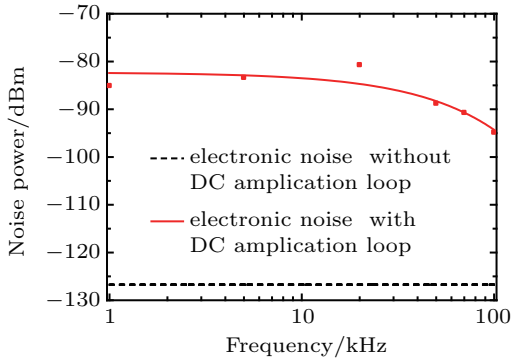


Fig. 3. Simulation curves of the electronic noises of the photodetector versus the analysis frequency with (red solid line) and without (black dashed line) the DC amplication branch.

2.2. SNR analysis

When two laser beams with equal power P are respectively injected into the two PDs of the BHD with the same responsivity of ρ, the illuminated photocurrents are given by

$$I_{\mathrm{PD1,Signal}} = I_{\mathrm{PD2,Signal}} = P \times \rho. \tag{15}$$

Their corresponding current densities are expressed as

$$\Delta i_{\mathrm{PD1,Signal}} = \sqrt{2qI_{\mathrm{PD1,Signal}}\Delta f}, \tag{16}$$

$$\Delta i_{\mathrm{PD2,Signal}} = \sqrt{2qI_{\mathrm{PD2,Signal}}\Delta f}. \tag{17}$$

According to the principle of BHD, the total current spectral density is expressed as

$$\Delta i_{\mathrm{PD,Signal}} = \sqrt{4qI_{\mathrm{PD1,Signal}}\Delta f}. \tag{18}$$

By multiplying Eq. (18) with the gain impedance $|Z_{\mathrm{s}}|$, the signal intensity is given by

$$e_{\mathrm{Signal}} = \Delta i_{\mathrm{PD,Signal}} \cdot |Z_{\mathrm{s}}|. \tag{19}$$

Thus the SNR of the photodetector can be expressed as

$$\mathrm{SNR} = 10\lg(e^2_{\mathrm{Signal}}/e^2_{\mathrm{El,Noise}}). \tag{20}$$

Substituting Eqs. (14) and (19) into Eq. (20), a general expression for simulating the SNR is deduced as

$$\mathrm{SNR} = 10\lg\left[\frac{(\Delta i_{\mathrm{PD,Signal}})^2 \cdot |Z_{\mathrm{s}}|^2}{(4KT/R_{\mathrm{f}}) \cdot |Z_{\mathrm{s}}|^2 \cdot \Delta f + e^2_{\mathrm{in}} \cdot |Z_{\mathrm{n}}|^2 \cdot \Delta f}\right]. \tag{21}$$

According to Eq. (21), the feedback resistor plays a major role in the SNR of the detector without the DC amplification branch. However, the self-oscillation of the photodetector becomes possible with the increase of the feedback resistor. A feedback resistor of 200 kΩ is adopted to improve the SNR under non-oscillatory premise. A parallel capacitor of 0.5 pF is used to compensate the transfer phase delay. It is worth noting that the signal at audio-frequency band is more vulnerable to couple into the DC amplification branch. As a result, the signal shunting into the AC amplification branch becomes weaker as the frequency decreases. Thus, the SNR of the photodetector without the DC amplification branch is far larger than that with the DC amplification branch at audio-frequency band.

3. Experimental setup and results

We design and build the BHD with focus on measuring the bright squeezed light in the frequency range from 1 kHz to 100 kHz. The scheme, shown in Fig. 4, is constructed to test the performance of the photodetector. The laser source is a home-made single-frequency Nd:YVO_4 laser at 1064 nm with the maximum output power of 2 W, its output power can be conveniently adjusted by a power adjustment system consisting of a half-wave plate (HWP1) and a polarization beam splitter (PBS1). The output beam of PBS1 is injected into the electro-optic amplitude modulator (EOAM), which is modulated by a signal generator connected with its RF input connector. The PBS2 in combination with the EOAM serves as amplitude modulation. The most important optical component is a 50/50 beam splitter consisting of HWP2 and PBS3, which can be used to finely tune the splitting ratio by rotating the HWP2. The output beams from the PBS3 are injected into two PDs integrated in the BHD after being focused with lenses L1 and L2. The DC output of the photodetector is connected with a digital oscilloscope (OSC) to verify whether the lights are thoroughly received by each PD and meanwhile make sure the powers of the lights injected into each PD are equal. The AC output is connected with a spectrum analyzer (FSW-8) to read the noise power. In our photodetector, two InGaAs PDs (G8376-03) with the same performance parameters are used as the optical receivers.

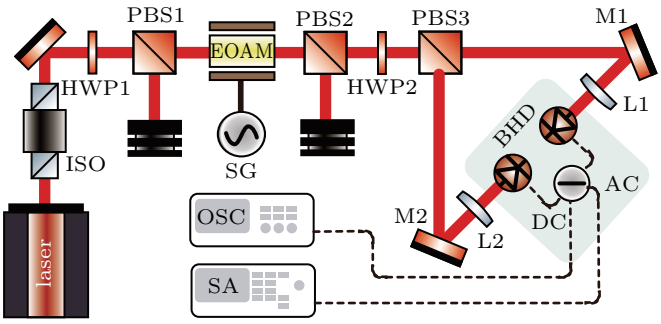


Fig. 4. Experimental setup for measuring the performance of the photodetector. ISO: isolator; HWP: half-wave plate; PBS: polarization beam splitter; EOAM: electro-optic amplitude modulator; SG: signal generator; BHD: balanced homodyne detector; OSC: oscilloscope; SA: spectrum analyzer.

Firstly, the SNRs of the photodetector with and without the DC amplification branch are measured. Changing the laser power from 125 μW to 8 mW by a factor of two, the measured results with and without the DC amplification branch are shown in Figs. 5(a) and 5(b), respectively. The experimental results confirm that the electronic noise without DC amplification branch is far less than that with DC amplification branch. The change trend of the electronic noise is in good agreement with the theoretical predication. It is worth noting that the noise power with the DC amplification branch is independent of the laser power in the range from 1 kHz to 20 kHz due to the AC signal at the frequency band bypassed to the DC branch. Meanwhile, the SNR increases with the analysis frequency. There are two reasons: one is the reduction of the electronic noise, and the other is the signal proportion increase through the AC branch. However, the noise power without the DC amplification branch entails a 3-dB shift of the corresponding noise trace when changing the laser power by a factor of two. The results indicate that the photodetector operates linearly in the measurement regime. When the total laser power injected

into the PDs equals to 2 mW, the photodetector demonstrates a clearance of more than 30 dB between the quantum noise and the electronic noise in the frequency region without noise peak. A maximum clearance of 48 dB at 60 kHz is achieved when 8 mW laser is illuminated into each PD. Thus, by adding a switch at the DC branch and a capacitance at the AC branch, the electronic noise of the AC branch is effectively reduced, the SNR of the AC branch is significantly increased, and the saturation problem of the AC branch is overcome for the detection of the bright squeezed light. In addition, the DC branch does also provide a monitor signal for laser beam alignment.

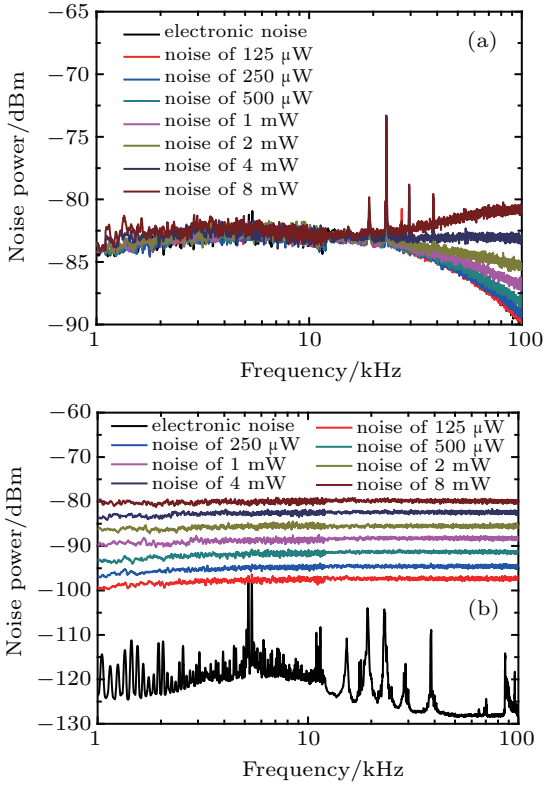


Fig. 5. The SNRs of the photodetector (a) with and (b) without the DC amplication branch measured at several incident powers. The traces are pieced together from two FFT frequency windows: 1–12 kHz, 12–100 kHz. Each point is the averaged rms value of 16 measurements. The RBWs of the two windows are 30 Hz and 100 Hz, respectively.

Secondly, according to Ref. [2], the deviation between the measured and real squeezed degrees grows with the increase of the LO intensity noise, but the CMRR of the photodetector can eliminate the impact of the LO intensity noise, which is dependent on the level of the CMRR. The CMRR is another important factor for the performance evaluation of the photodetector, which shows the performance of eliminating the influence of classical noise from the local oscillator. The CMRR is defined as the ratio between the common mode signal and the differential mode signal. The results of CMRR are shown in Fig. 6. The CMRR is higher than 59 dB in the frequency range from 1 kHz to 100 kHz. The inset shows the CMRR of 59.5 dB at the analysis frequency of 6.1 kHz.

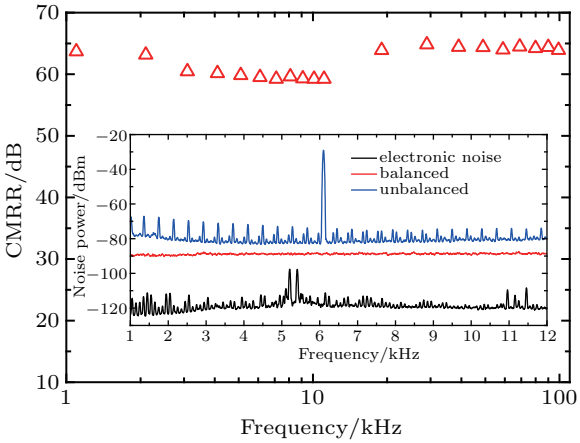


Fig. 6. The CMRR of the photodetector without the DC ampliation branch versus the analysis frequency at the incident power of 1 mW.

4. Conclusion and perspectives

We have developed a low-noise, high-gain BHD based on the TIA technology and the *L*–*C* combination for the measurement of the bright squeezed state in the range from 1 kHz to 100 kHz. A capacitance is mounted at the input end of the AC branch to prevent the DC photocurrent from entering the AC branch and avoid AC branch saturation. By adding a switch at the DC branch, the DC branch can be flexibly turned on and off on different occasions. When the switch is on, the DC output provides a monitor signal for conveniently aligning the laser beams to the PDs. When the switch is off, the electronic noise of the AC branch is greatly reduced at audio-frequency band due to immunity to the impedance of the DC branch, hence the SNR of the AC branch is significantly improved. As a result, the electronic noise of the AC branch is close to −125 dBm, and the maximum SNR of the AC branch is 48 dB for 8 mW incident power in the range from 1 kHz to 100 kHz. The noise power without the DC amplification branch entails a 3-dB shift of the corresponding noise trace when changing the laser power by a factor of two, indicating that the photodetector operates linearly in the measurement regime. The CMRR of the AC branch is higher than 59 dB in the frequency range from 1 kHz to 100 kHz. The developed photodetector paves a path for measuring the bright squeezed state at audio-frequency band.

References

[1] Hou L L, Xue J Z, Sui Y X and Wang S 2019 *Chin. Phys. B* **28** 094217
[2] Yang W H, Jin X L, Yu X D, Zheng Y H and Peng K C 2017 *Opt. Express* **25** 24262
[3] Yu X D, Li W, Zhu S Y and Zhang J 2016 *Chin. Phys. B* **25** 020304
[4] Du J S, Feng J X, Ma Y Y, Li Y J and Zhang K S 2018 *Acta Sin. Quantum. Opt.* **24** 14
[5] Feng Y Y, Shi R H and Guo Y 2018 *Chin. Phys. B* **27** 020302
[6] Schnabel R, Mavalvala N, McClelland D E and Lam P K 2010 *Nat. Commun.* **1** 121
[7] The L I G O Scientific Collaboration 2011 *Nat. Phys.* **7** 962
[8] Cella G and Giazotto A 2011 *Rev. Sci. Instrum.* **82** 101101
[9] Abbott B P 2016 *Phys. Rev. Lett.* **116** 061102

[10] Abbott B P 2017 *Phys. Rev. Lett.* **118** 221101
[11] Polzik E S, Carri J and Kimble H J 1992 *Phys. Rev. Lett.* **68** 3020
[12] Polzik E S, Carri J and Kimble H J 1992 *Appl. Phys. B* **55** 279
[13] Li Y Q, Lynam P, Xiao M and Edwards P J 1997 *Phys. Rev. Lett.* **78** 3105
[14] Li Y Q, Guzun D and Xiao M 1999 *Phys. Rev. Lett.* **82** 5225
[15] Ralph T C 1999 *Phys. Rev. A* **61** 010303
[16] Madsen L D, Usenko V C, Lassen M, Filip Radim and Andersen U L 2012 *Nat. Commun.* **3** 1083
[17] Stefszky M S, Mow Lowry C M, Chua S S Y, Shaddock D A, Buchler B C, Vahlbruch H, Khalaidovski A, Schnabel R, Lam P K and McClelland 2012 *Class. Quantum. Grav.* **29** 145015
[18] Appel J, Hoffman D, Figueroa E and Lvovsky A I 2007 *Phys. Rev. A* **75** 035802
[19] Liu Q, Feng J X, Li H, Jiao Y C and Zhang K S 2012 *Chin. Phys. B* **21** 104204
[20] Tian J F, Zuo G H, Zhang Y C, Li G, Zhang P F and Zhang T C 2017 *Chin. Phys. B* **26** 124206
[21] Zheng Y H, Wu Z Q, Huo M R and Zhou H J 2013 *Chin. Phys. B* **22** 094206
[22] Lu D M and Fan H Y 2014 *Chin. Phys. B* **23** 020302
[23] Masalov A V, Kuzhamuratov A and Lvovsky A I 2017 *Rev. Sci. Instrum.* **88** 113109
[24] Qin J L, Yan Z H, Huo M R, Jia X J and Peng K C 2016 *Chin. Opt. Lett.* **14** 122701
[25] Zhou H J, Yang W H, Li Z X, Li X F and Zheng Y H 2014 *Rev. Sci. Instrum.* **85** 013111
[26] Huang D, Fang J, Wang C, Huang P and Zeng G H 2013 *Chin. Phys. Lett.* **30** 114209
[27] Jin X L, Su J, Zheng Y H, Chen C Y, Wang W Z and Peng K C 2015 *Opt. Express* **23** 23859
[28] Wang S F, Xiang X, Zhou C H, Zhai Y W, Quan R N, Wang M M, Hou F Y, Zhang S G, Dong R F and Liu T 2017 *Rev. Sci. Instrum.* **88** 013107
[29] Zhou H J, Wang W Z, Chen C Y and Zheng Y H 2015 *IEEE Sensors. J.* **15** 2101
[30] Wang X Y, Bai Z L, Du P Y, Li Y M and Peng K C 2012 *Chin. Phys. Lett.* **29** 124202
[31] Valbruch H 2008 *Squeezed Light for Gravitationalwave Astronomy* (Ph.D. Dissertation) (Hannover: the Albert Einstein Institute and the Institute of Gravitational Physics of Leibniz Universitat Hannover) (in Germany)
[32] Wen X, Han Y S, Liu J Y, He J and Wang J M 2017 *Opt. Express.* **25** 020737
[33] Kay A 1988 *Photodiode Amplifier Noise Operational Amplifier Noise: Tech. Tips For Analyzing Reducing Noise* (1st Edn.)